THE ANNALS OF "DUNAREA DE JOS" UNIVERSITY OF GALATI
FASCICLE IX. METALLURGY AND MATERIALS SCIENCE
No. 2 - 2025, ISSN 2668-4748; e-ISSN 2668-4756
Article DOI: https://doi.org/10.35219/mms.2025.2.04

ON THE OPTIMIZATION OF MACHINED VSD POSITION FOR REPAIRED PIPES

Ionuţ LAMBRESCU
Universitatea Petrol-Gaze din Ploieşti, Bd. Bucureşti 39, Ploieşti, Romania
e-mail: ilambrescu@upg-ploiesti.ro

ABSTRACT

To be kept in use, pipelines with Volumetric Surface Defects (VSDs) must be evaluated and, if necessary, repaired. The first step in the repair process is machining the defect area. In all cases, the machined defect has a rectangular shape, with edges parallel/perpendicular to the pipe axis. We propose a novel approach: the VSD is scanned, the image is then processed using segmentation techniques, the VSD contour is detected, and finally, a family of rectangles with minimal area enclosing the VSD is defined. After that, a Finite Element Analysis is performed for each machined VSD, and an optimal case is selected.

KEYWORDS: pipes, volumetric defects, optimization

1. Introduction

The problem of pipelines with Volumetric Surface Defects (VSDs) is of great interest, since accidents involving pipelines transporting flammable or explosive fluids can have very serious consequences.

The general approach is to analyse the VSD and assess if the pipeline can be accepted as it is and allowed to continue operating, or it is necessary to apply a repair process that will enable the pipeline to remain in use for a specified period of time [1-4]. The repair process involves a machining phase, during which material in the area of the VSD is removed, followed by a repair phase, during which a material (the so-called filler) is used to fill the machined VSD, and the pipe is wrapped with a multilayer composite material [5].

In the literature that addresses this topic, the machined VSD is typically of rectangular shape, with the edges of the rectangle oriented parallel/perpendicular to the pipeline's axis [6].

In a previous paper, the author analysed the influence of the machined rectangular VSD on the stress and displacement distribution. The conclusion was that there exists a position of the machined VSD that produces a more favourable stress distribution [2].

The present paper aims to continue this analysis, this time starting from a real VSD, for which the objective is to find the most favourable dimensions and orientation of the rectangular machined VSD. The stages of the process are described in Figure 1.

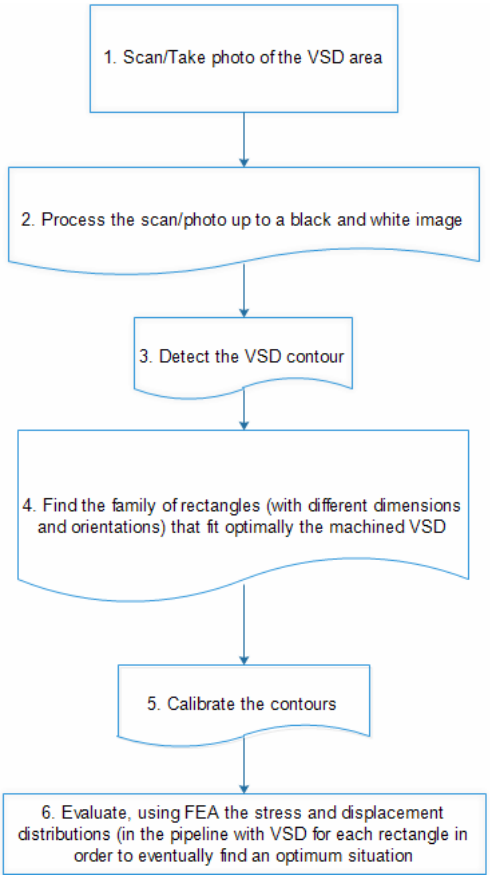

Fig. 1. *Stages of the proposed workflow*

THE ANNALS OF "DUNAREA DE JOS" UNIVERSITY OF GALATI
FASCICLE IX. METALLURGY AND MATERIALS SCIENCE
Nº. 2 - 2025, ISSN 2668-4748; e-ISSN 2668-4756
Article DOI: https://doi.org/10.35219/mms.2025.2.04

The first four stages of the workflow imply, apart from scanning [7, 8] or taking a picture of the area of the pipeline with a VSD, writing a script that will accomplish stages 2, 3, and 4 in the workflow.

Stage 5 involves the calibration process, since the rectangles resulting from stage 4 have dimensions expressed in pixels. These dimensions must be converted to dimensions expressed in millimeters (mm). This is the process we call calibration. Details on how this is done will be given later in the paper.

Stage 6 involves performing finite elements analysis for each scenario (a scenario corresponds to a rectangle with specific dimensions and orientation). In the end, we will ultimately obtain an optimal solution -that is, the case with the smallest values for stresses.

2. Image processing

Figure 2.a presents an image obtained through a 3D scanning process (the image shows only the region containing the VSD, which has been isolated from a pipeline with an outer diameter of 508 mm and a wall thickness of 10 mm). The scan was performed using an HP 3D Structured Light Scanner Pro 3 [9].

The image was converted to black and white (bw) format, as presented in Figure 2.b. All image processing was performed in Matlab [10, 11].

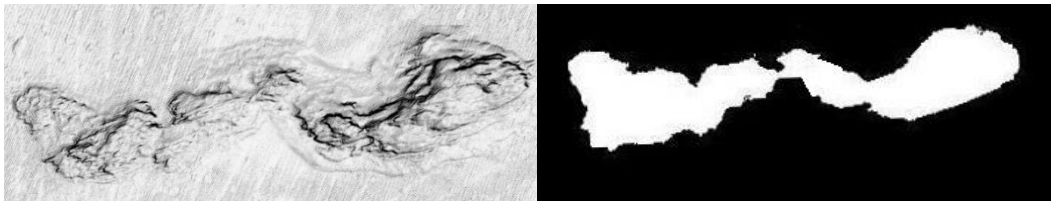

a) Initial scanned image *b) Processed image (bw)*

Fig. 2. *Images with VSD*

2.1. Determination of the family of rectangles

The bw image serves as an input for the process of determining a family of rectangles that will fit (enclose) the boundary of the VSD. Each rectangle will fit the boundary of the VSD and will have edges parallel/perpendicular to variable directions that pass through the centroid of the VSD area. Essentially, this results in a family of rectangles that rotate around a central point. This point is the centroid of the VSD area, and it is identified by our application using image segmentation techniques [12, 13]. For better understanding see Figure 3.

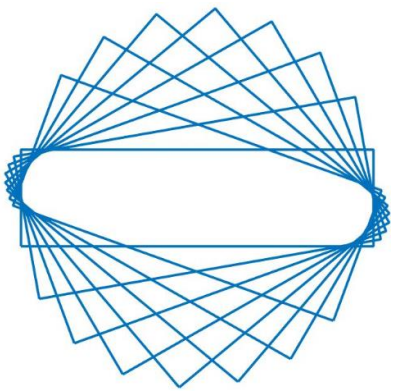

Fig. 3. *Family of rectangles*

In order to better understand the following explanations, Figure 4 presents the VSD as it appears on the pipeline. In the same image, a bounding rectangle is shown at a position tilted by 10 degrees.

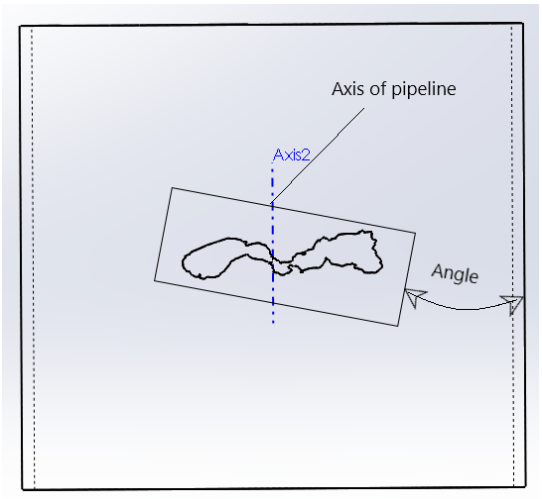

Fig. 4. *VSD and a bounding rectangle*

Figure 5 presents the first 4 bounding boxes for the VSD shown in Figure 2, starting from a direction tilted at 0 degrees and ending with one tilted at 30 degrees.

It should be noted that when the bounding rectangles were generated, we applied a covering

THE ANNALS OF "DUNAREA DE JOS" UNIVERSITY OF GALATI
FASCICLE IX. METALLURGY AND MATERIALS SCIENCE
N°. 2 - 2025, ISSN 2668-4748; e-ISSN 2668-4756
Article DOI: https://doi.org/10.35219/mms.2025.2.04

tolerance of 7%. This was necessary since some of the calculations performed during the process produced non-integer values, while coordinates within the image must be integer values. This is a source of small errors that must be compensated.

The VSD presented in Figure 2 also has a special characteristic. It is placed on the pipeline such that its minimum bounding box (the minimum bounding box is a property of the VSD area, determined using image segmentation techniques) has edges that are parallel or perpendicular to the pipeline's axis. The dimensions and position of the minimum bounding box are intrinsic properties of the VSD area as an image region, while for all other rectangles, edge orientation is constrained. For these rectangles, the dimensions are resulting parameters, determined after the orientation is fixed.

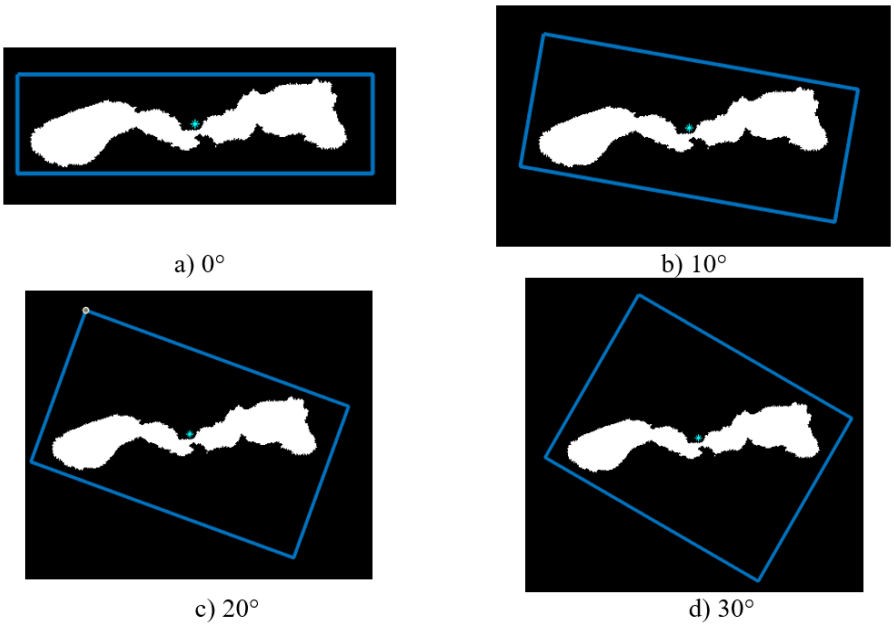

a) 0° b) 10° c) 20° d) 30°

... and other 4 positions up to 70°

Fig. 5. *Bounding rectangles*

3. Finite Element Analysis

For the eight rectangles we obtained (from 0 degrees to 70 degrees, in 10-degree steps), we performed a finite element analysis in order to determine if we can identify a most favourable configuration (in terms of stress values) [14-19].

The analysis was performed using Ansys Mechanical [20].

As shown in Figure 6, each rectangle serves as the starting point for the machining of the VSD. The machined VSDs include fillet radii and depths that depend on the depth of the original VSD. In our case, the VSD depth was 7.5 mm.

The results obtained for the VSD depicted in Figure 2 are presented in Figure 7. For each orientation of the machined VSD, we present the values for Von Mises stress, circumferential stress, and radial displacements, respectively.

As can be seen in Figure 7, the values for all the considered parameters reach their minimum for the bounding rectangle tilted at 0 degrees (it is in fact the minimum bounding box of the VSD contour). At this stage, we emphasize that the relative variation for all three parameters is significant: 55% for Von Mises stress, 45% for circumferential stress, and 72% for radial displacement, respectively.

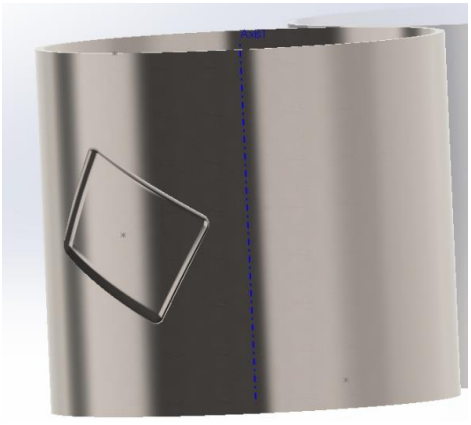

Fig. 6. *Machined VSD for one of the analysed positions*

THE ANNALS OF "DUNAREA DE JOS" UNIVERSITY OF GALATI
FASCICLE IX. METALLURGY AND MATERIALS SCIENCE
No. 2 - 2025, ISSN 2668-4748; e-ISSN 2668-4756
Article DOI: https://doi.org/10.35219/mms.2025.2.04

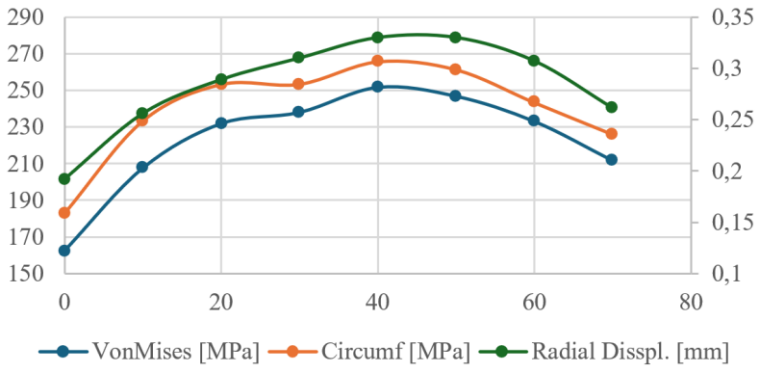

Fig. 7. *Comparison between positions of the machined VSDs*

Because the first VSD considered had a particular orientation on the pipeline, we also analysed another VSD. Its position on the pipeline is presented in Figure 8.a.

In Figures 8.b-f, one can see the bounding rectangles obtained with our code, again for angles ranging from 0 degrees to 70 degrees, in 10-degrees increments.

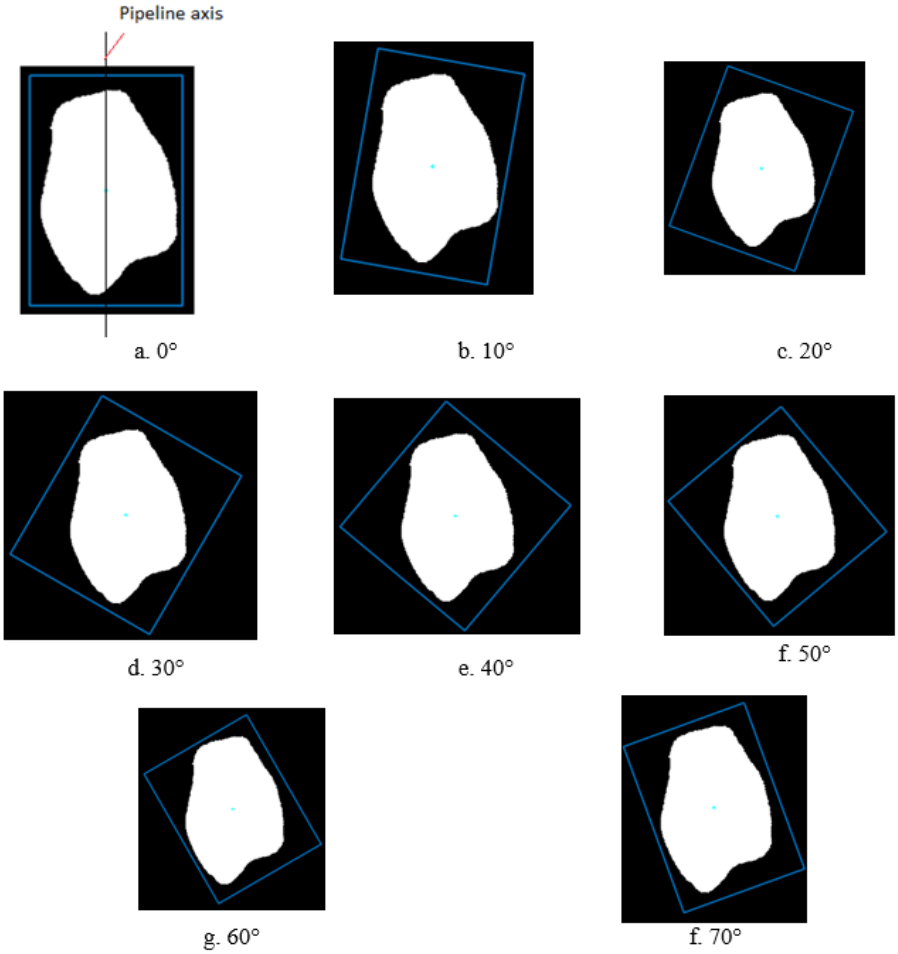

Fig. 8. *Bounding rectangles for another VSD*

In this case, the results are presented in Figure 9. This time it is obvious that for tilting angles of 40, 50, and 60 degrees, one obtains significantly lower values for all the three considered parameters.

THE ANNALS OF "DUNAREA DE JOS" UNIVERSITY OF GALATI
FASCICLE IX. METALLURGY AND MATERIALS SCIENCE
Nº. 2 - 2025, ISSN 2668-4748; e-ISSN 2668-4756
Article DOI: https://doi.org/10.35219/mms.2025.2.04

The relative variation of these parameters over the angle range is as follows: 30.5% for Von Mises stress, 34.1% for circumferential stress, and 9% for radial displacement respectively

Another interesting observation is that by modifying the tilting angle, the locations of maximum stress values (Von Mises or circumferential) is registered in different VSD areas. Figure 10.a for example presents the Von Mises stress distribution (for the second VSD) with a bounding rectangle tilted at 0 degrees (the minimum bounding box), while Figure 10.b shows the same parameter for a bounding rectangle tilted at 40 degrees. It is clear that the region with high stress values is smaller in the latter case.

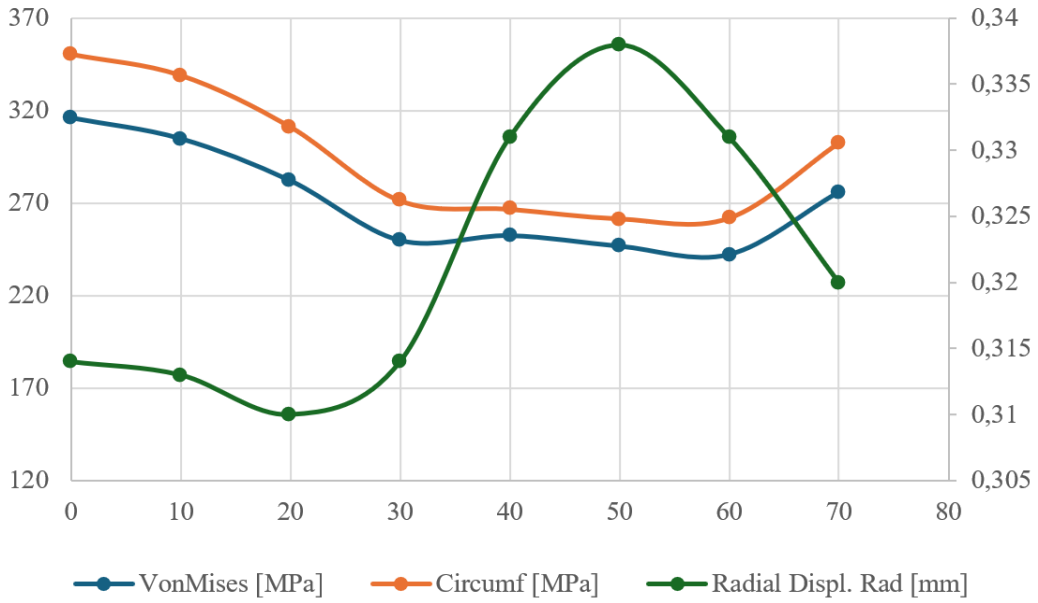

Fig. 9. *Comparison between positions of the machined VSDs from Figure 8*

Figure 11 presents the variation of the three parameters with the tilting angle, with two curves added. These curves are obtained for a value of the fillet angle of the machined VSD of 20 mm (instead of 15 mm). We can see that for tilting angles of 40 and 50 degrees, there are relative differences of 3%.

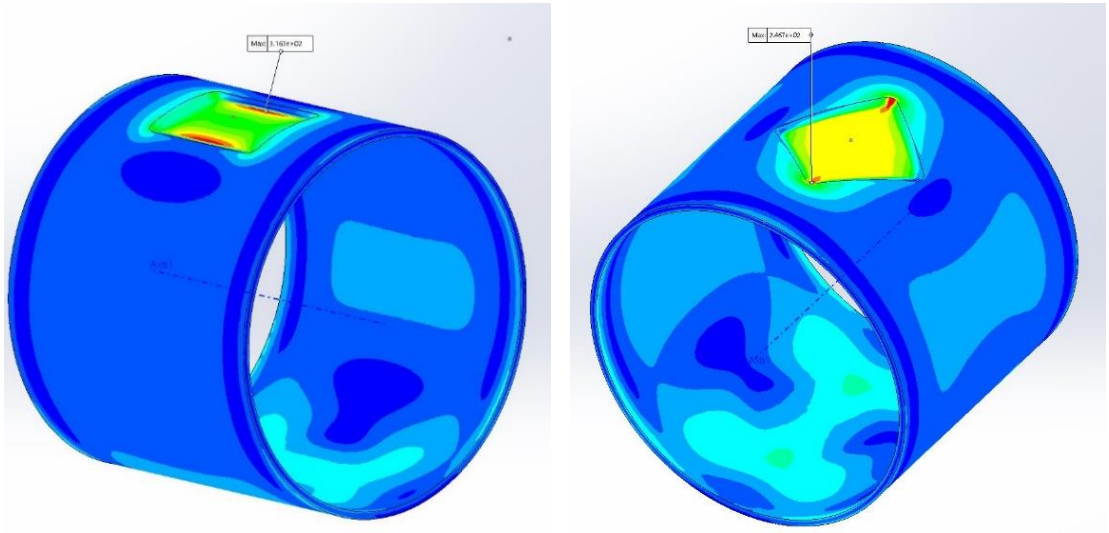

a) Von Mises stress 0 degrees *b) Von Mises stress 40 degrees*

Fig. 10. *Comparison between positions of the maxima Von Mises stress areas*

THE ANNALS OF "DUNAREA DE JOS" UNIVERSITY OF GALATI
FASCICLE IX. METALLURGY AND MATERIALS SCIENCE
No. 2 - 2025, ISSN 2668-4748; e-ISSN 2668-4756
Article DOI: https://doi.org/10.35219/mms.2025.2.04

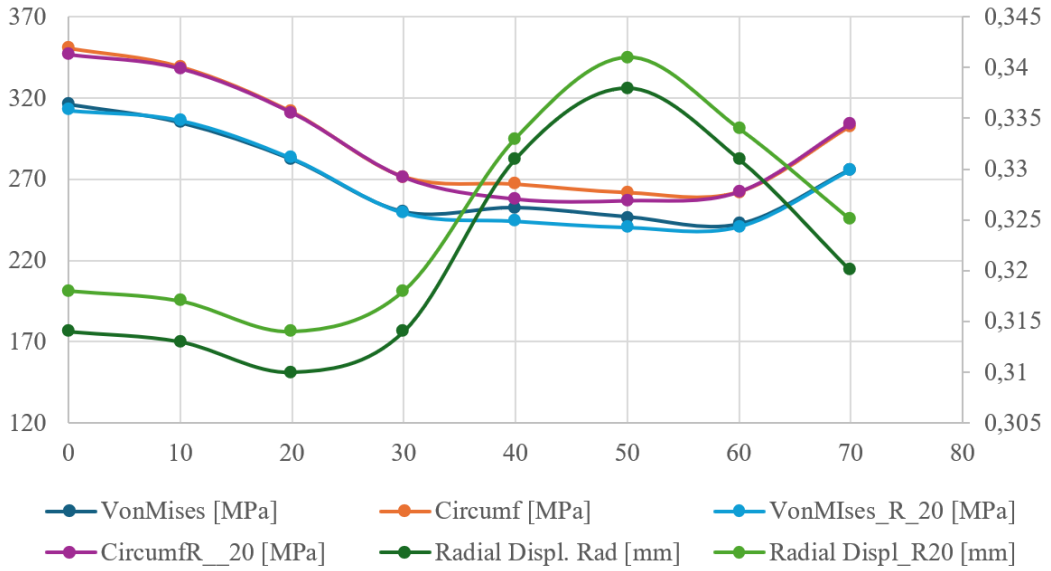

Fig. 11. *Comparison between positions of the machined VSDs from Fig. 8 including cases with fillet radius of 20 mm*

4. Conclusions

Practically all studies [1, 19, 21, 22] (and the references can be extended) dealing with repaired pipes containing VSDs consider the machined VSD to be rectangular, with edges parallel/perpendicular to the pipe axis. However, there are cases where, due to the VSD shape, the resulting machined area becomes very large, this implying not only the fact that the pipe is weakened, but also the time for machining the VSD is increasing. What the author is proposing is a method to identify the optimal rectangular shape for the machined VSD – one that circumscribes the unprocessed defect but has edges inclined to the pipe axis. The best machined VSD is selected through finite element analysis of multiple VSD orientations. The optimal rectangle is the one that "produces" the most favourable stress, strain, or displacements in the pipe with machined VSD. The analysis performed showed that both the dimension and position of the machined VSD significantly influenced the stress/strain distribution in the pipe (with differences of up to more than 30% for Von Misses stresses).

Furthermore, the shape and orientation of the bounding rectangle also influence the area where the stress exhibits maximum values (see Fig. 10). This detail is of paramount importance, as it can be correlated with the fillet radius applied at the VSD bottom to help identify regions with high failure risk.

The proposed method can be sped up using parametrization techniques in generating the geometric model of the pipe with machined VSD.

Because the finite element analysis performed is static structural (linear), the overall duration of the process is reduced.

We believe that the advantages offered by the proposed method, in terms of increased repaired pipe resistance and reduced machining time, makes this research valuable to professionals working in the field.

References

[1]. Yeom K. J., *et al.*, *Integrity Assessment of a Corroded API X70 Pipe with a Single Defect by Burst Pressure Analysis*, Engineering Failure Analysis, vol. 57, p. 553-561, November 2015.
[2]. Lambrescu I., Dinita A., Minescu M., *About the Influence of the Corrosion Defect Geometry on Repaired Pipes Stress Distribution*, J. Pressure Vessel Technol., 143(1), 011802, /doi.org/10.1115/1.4047877, Feb 2021.
[3]. Chebakov M. J., *et al.*, *Experimental and Numerical Research on Renovated Pipeline Prototype with Durface Defect, Non-destructive Testing and Repair of Pipelines*, E. N. Barkanov, A. Dumitrescu, I. A. Parinov, eds. Springer International Publishing AG, Cham, Switzerland, p. 353-368, 2018.
[4]. Su C.-I., Li X., Zhou J., *Failure Pressure Analysis of Corroded Moderate-to-High Strength Pipelines*, China Ocean Engineering, vol. 30, issue 1, p. 69-82.
[5]. ***, *ISO 24817:2015. Petroleum, petrochemical and natural gas industries — Composite repairs for pipework — Qualification and design, installation, testing and inspection*.
[6]. Barkanov E. N., Dumitrescu A., Parinov I. A., *Non-destructive Testing and Repair of Pipelines*, Springer International Publishing AG, Cham, Switzerland.
[7]. Lambrescu I., Dinita A., Minescu M., *Considerations on the Evaluation and Management of Volumetric Surface Defects on Pipelines Using 3D Scanning and Finite Element Analysis*, Revista de chimie, 71 (4), p. 19-28, 2020.
[8]. Lambrescu I., Minescu M., Dinita A., *Implementing of 3D Scanning Techniques in the Analytical and Numerical Assessment of Pipelines with Volumetric Surface Defects*, Revista de Chimie, 70, no. 12, 2019.

[9]. ***, https://support.hp.com/us-en/product/details/hp-3d-structured-light-scanner/model/14169439.
[10]. Song Y. Q., Gao C. Y., *Application of MATLAB on Moire image processing*, Proceedings of the 5th International Conference on Nonlinear Mechanics, p. 854-856, 2007.
[11]. Magrab E. B., *et al.*, *An Engineer's Guide to MATLAB, 3e: with Applications from Mechanical, Aerospace, Electrical, and Civil Engineering*, Prentice Hall, 2011.
[12]. Tewari P., Surbhi P., *Evaluation of some recent Image segmentation method's*, 3rd International Conference on Computing for Sustainable Global Development (INDIACom), Proceedings of the 10th Indiacom, 3rd International Conference on Computing for Sustainable Global Development, p. 3741-3747, 2016.
[13]. Song Y. H., Yan H., *Image Segmentation Techniques Overview*, Asia Modelling Symposium (AMS) / 11th International Conference on Mathematical Modelling and Computer Simulation, p. 103-107, 2017.
[14]. Jungyeom K., *et al.*, *Integrity assessment of a corroded API X70 pipe with a single defect by burst pressure analysis*, Engineering Failure Analysis, vol. 57, p. 553-561, November 2015.
[15]. Zienkiewicz O. C., Taylor R. L., *Finite Element Method for Solid and Structural Mechanics*, Sixth Edition. Elsevier BH, Oxford, UK, 2006.
[16]. Nasedkina A. A., *et al.*, *Static Finite Element Analysis of a Pipeline with Volumetric Surface Defects Using MPC Approach*, International Conference on Physics and Mechanics of New Materials and their Applications (PHENMA 2015), At Azov, Russia.
[17]. Chiodo M. S., Ruggieri C., *Failure assessments of corroded pipelines with axial defects using stress-based criteria: Numerical studies and verification analyses*, International Journal of Pressure Vessels and Piping, 86, p. 164-176, 2009.
[18]. Liu H., Khan F., Thodi P., *Revised burst model for pipeline integrity assessment*, Engineering failure analysis, 80, p. 24-38, 2017.
[19]. da Costa Matos H. S., *et al.*, *Failure Analysis of Corroded Pipelines Reinforced with Composite Repair Systems*, Engineering Failure Analysis, vol. 59, p. 223-236, 2016.
[20]. *, *ANSYS – Finite Element Analysis, Release 19.0 User Guide*, 2018.
[21]. Lim K. S., *et al.*, *Behaviour of Steel Pipelines with Composite Repairs Analyzed using Experimental and Numerical Approaches*, Thin-Walled Structures 139, p. 321-333, 2019.
[22]. Noor N., *et al.*, *An Overview of Corroded Pipe Repair Techniques Using Composite Materials*, International Journal of Chemical, Molecular, Nuclear, Materials and Metallurgical Engineering. vol. 10, no. 1, p. 19-25, 2016.